Journal of Petroleum Science and Technology 12(1): 33, 2022, Pages 2-20
DOI:10.22078/JPST.2022.4845.1809

Journal of Petroleum Science and Technology

Research Paper

https://jpst.ripi.ir/

Application of Pressure-Volume (P-V) Fractal Models in Modeling Formation Pressure and Drilling Fluid Determination in an Oilfield of SW Iran

Pooria Kianoush[1], Ghodratollah Mohammadi*[1], Seyed Aliakbar Hosseini[2], Nasser Keshavarz Faraj Khah[3] and Peyman Afzal[1]

1. Department of Petroleum and Mining Engineering, South Tehran Branch, Islamic Azad University, Tehran, Iran

2. Department of Petroleum, Materials and Mining Engineering, Central Tehran Branch, Islamic Azad University, Tehran, Iran

3. Geoscience Faculty, Research Institute of Petroleum Industry (RIPI), Tehran, Iran

Abstract

Accurate knowledge of pore and fracture pressures is essential for drilling wells safely with the desired mud weight. By definition, overpressure occurs when the pore pressure is higher than the normal hydrostatic pressure and is associated with specific environmental conditions in a particular part of the earth. This study focuses on the formation pressure studies' domain for an oilfield in SW Iran. It generally consists of carbonate rocks with no shale interbeds except for the Kazhdumi Formation. This study is based on information from 23 wells and the interpretation of seismic data. The effective, pore, and fracture pressure models are determined from combined geostatistical models and compared with fractal models. The highest correlation between the final effective pressure cube and the velocity cube is related to the lower Fahliyan Formation with 86% and Ilam with 71%, which indicates the accuracy of the modeled data with the original data. Based on the final formation pressure cubes, the maximum pore pressure is 10,000 psi in the Gadvan Formation up to the upper Fahliyan Formation, and the maximum fracture pressure is 13,000 psi in the lower Fahliyan up to the Gotnia Formation. Based on the Logratio matrix obtained from the pressure-volume (P-V) fractal model, the maximum overall accuracy (OA) in the dominant limestone intervals is 0.74 at depths of 2000-3000 meters, which is related to the Asmari to Sarvak Formations. Furthermore, it indicates a high correlation of the pore pressure cube model obtained from the combination of sequential Gaussian simulation (SGS) and co-kriging models with acoustic impedance inversion (AI) for minimizing the time and cost of drilling in new wells of the studied field.

Keywords: Seismic Velocity Model, Sequential Gaussian Simulation, Formation Pressure Cube, Pressure-volume (P-V) Fractal Model, Logratio Matrix.

Introduction

Understanding the pore pressure of the formation is essential for the safe and economical drilling of wells and for assessing exploration risk factors such as formation migration fluid and sediment integrity. Usually, before drilling, an initial estimate of the pore pressure is made using surface seismic data; in this method, mainly seismic velocity is used. Therefore, the accuracy of the velocity models used to determine the pore pressure is of utmost importance. Using seismic data is the only method to predict the pore pressure in the pre-drilling stage. It estimates the pore pressure based on the effect of wave velocity on pressure changes [1-4].

Seismic data, well logs, drilling information, and basin modeling are required to determine the pore pressure gradient in a field. Suppose there is a lack of necessary information in a particular field area. In that case, the necessary well logs are prepared using estimating models after screening the available data and preparing the database [5-9]. One way to control the values of the sonic logs is to match them with the values obtained from seismic velocity analysis. The theory of quantitative evaluation of the internal pressure of the earth using acoustic instruments depends on the amount of porosity. Therefore, sonic logs can be a good indicator of the internal pressure of the ground, i.e., increasing the sound passage time in the zones is a function of changing the porosity or increasing the pore pressure gradient. So we can identify areas with abnormal pore pressure and reduce drilling risk and related costs. Because in addition to pressure, other factors such as lithology also affect the speed of seismic waves; therefore, using available geological information and well logs can prevent errors in estimating the formation pressures, especially in

**Corresponding author:* Ghodratollah Mohammadi, *Department of Petroleum and Mining Engineering, South Tehran Branch, Islamic Azad University, Tehran, Iran*
E-mail addresses: ghodratollah46@gmail.com
Received 2022-06-28, Received in revised form 2022-10-13, Accepted 2022-10-18, Available online 2022-12-13

carbonate formations [1,3, 7-11]. It is necessary to calculate the shear velocity to estimate the fracture pressure of the formation. Determining the shear wave velocity by methods such as core analysis requires a lot of time and money. Due to the lack of sufficient cores, lithological changes, and reservoir heterogeneity, determining this parameter by conventional methods is not very accurate. Also, many experimental relationships have been presented regarding the calculation of shear wave velocities, the most widely used method proposed by Castagna in 1993 based on lithological changes [12-13]. Intelligent methods are one of the new methods with low cost and high accuracy. Using petrophysical graphs such as DSI, they can estimate the shear wave velocity of the reservoir in the shortest possible time [14-15]. The conventional method for calculating the pore pressure in the reservoir range is the Bowers method. An effective stress cube is generated using the relationship between velocity and effective stress (Equation 1). The above relationship is proposed in sediments under normal pressure as follows [16-17]:

$$V = V_0 + A\sigma^B \quad (1)$$

where V_0 is the velocity of unconsolidated fluid-saturated sediments, and A and B describe the variation in velocity with an increase in effective stress (σ), and it can be derived from offset well data [16-18].

To calculate the effective pressure in the reservoir area using the Bowers relation, the relation coefficients must first be obtained. Thus, according to the effective pressure information at wells (MDT/RFT/DST) and the overburden pressure cube created in the previous section, the effective stress at points of these wells can be calculated [19-23].

Sequential Gaussian simulation (SGS) is typical in geostatistical simulations, and in many simulators, it has responded to porosity, permeability, and other regional variables. In this method, the simulated value at each point is obtained using the probability distribution function calculated from the raw data and the previous simulation data in the nearest neighbors of the desired point. The first principle in all Gaussian methods is the normality of the raw data; otherwise, they must become the standard [24-25]. In the co-kriging method, the evaluation is performed using the correlation between the desired regional variable and the auxiliary variable in places with a shortage of samples. If the correlation between the two variables is greater than 0.5, the estimation error is significantly reduced by this method [26-27]. Also, in 2018, it has been shown by Karmi et al. that among the different geostatistical models for the same data, the co-kriging method has the highest correlation coefficient with a minimum allowable error of 0.5 [26-28].

Fractal geometry methods are mainly used to analyze complex shapes of geological structures, especially in structural geology and engineering branches, and the separation of geochemical and mineralogical communities, especially in economic geology, mining and geophysics. Among these methods, grade-area, grade-number, and power-area spectrum methods are very useful in earth sciences.

Mandelbrot and Agterberg proposed a value-size method for determining threshold values and geochemical backgrounds. Afzal drew a logarithmic diagram of Grade-Volume wherever the slope of the curve has changed drastically, i.e., the statistical population has changed. That indicates a sharp change in grade and a function of changing geological and mineralization conditions [29-38].

A logarithmic matrix has been used to investigate the overall accuracy between geological and mathematical models. Caranza first proposed this matrix in 2011 in gold anomalies caused by stream sediments in the northwest Philippines. A 2-by-2 matrix is used to do this. Any data with the highest overlap has the results of geological and mathematical models after calculating the overall accuracy (OA) can be considered a definite result with the least amount of error [39-40]. Three-dimensional modeling and visualization of subsurface petroleum reservoirs is a critical industry practice, and its significance originates from its theoretical and application value in exploration, development, and production. When modeling the subsurface system in both conventional and unconventional resources is modeled, it is critical to take into account a large number of datasets. The more data entered into the model, the better the model's accuracy is. The heterogeneity of the data, the time required for data handling, numerical storage and accessibility, and the reliability of geological information assessments could all be sources of uncertainty that impact the 3D modeling process, posing modeling challenges. Such 3D modeling challenges can be overcome with more integrated data, precise calibration, and core measurements, resulting in more precise models [41].

In the study area located in the south Azadegan Field, out of 42 wells available, 23 wells have the most selected information, of which 17 wells located in the central, western, and southern parts have effective pressure test data in the Ilam to Fahliyan reservoir Formations. It is discontinuous, but these data do not exist in the field's side sections. This log must be estimated for the wells in the side sections to calculate the pore pressure gradient in the whole field. For this purpose, by determining the relationships between the existing reservoir data, the initial data cube with geostatistical methods such as Sequential Gaussian Simulations (SGS) and co-kriging with the exact coordinates and inverse distance method has been modeled.

Reservoir data include compressional and shear velocity, density, gamma, porosity, fluid saturation logs, interval seismic migration velocity, and acoustic impedance resulting from seismic inversion. South Azadegan Field formations are modeled based on the interpretation of time-domain seismic horizons data and correlated with geological information obtained from exploratory drilling. Depth-domain seismic horizons have been constructed as separate surfaces from the surface Aghajari Formation to the Gotnia Formation. The geological model has been built with a simple network of Petrol 2016 software.

The general purpose of conducting this study is to determine the final model of the drilling mud window for conducting new drilling in the entire area of the studied field with the highest possible compatibility. It has been carried out in three stages, including models of interval velocities, formation pressures, and finally, determining the range of drilling fluid weight. This manuscript is the result of the 2nd part of the studies.

In this article, the combination of geostatistical methods of the SGS and co-kriging with the AI was used for the first time to construct the final models of the formation pressure cube in the entire area of South Azadegan Field. Also, other innovations of the present research include using new capabilities of Petrel 2016 software for conditional programming, including sequential and nested conditional expressions to combine logs and cubes into a single model and remove out-of-range values. And finally, use the pressure-volume fractal models to separate the pressure regimes of the formation and carry out the matching of mathematical models of pressure regimes and geological models in the form of dominant lithology and validation of the studies in the acceptable range for the first time.

Geological Setting

Geological Model Based on Seismic Interpretation

The Azadegan oil field is located in the transition zone between the Arabian plate and the Zagros basin, which is relatively far from the Zagros zone. The Zagros orogeny has changed the shape and fracture of the subsurface layers due to the presence of shale and marl in the Cenozoic Formations (Gurpi and Pabdeh) and the reduction of tectonic stress. Although they still have a sealing role in restraining the migration and vertical loss of oil [42].

The Abadan Plain comprises three main deep-seated trends: NE-SW, N-S, and NW-SE. The NE-SW trending Hendijan high and the N-S trending Burgan-Azadegan high are the region's most prominent structural features, extending north within the Zagros Fold-thrust belt structures (ZFTB) [43-44]. The seismic profile across Azadegan high shows a steep fault system in the Jurassic and underlying sedimentary rocks. The onlapping reflectors, especially on the western flank, and thinning of the layers above the crest indicate the uplift of the Azadegan high during the Upper Cretaceous. Geological interpretation of the Azadegan high showed the steep faults die up section [43-45].

The Azadegan and Mehr structures and several oilfields are located along with the regional trend in Saudi Arabia, Kuwait, and Iraq, as seen in Figure 1. In SW Iran, the N-S trend can be identified in the Abadan Plain and the Dezful Embayment. The Asmari Formation shows local thinning in the crest of the Azadegan Anticline. In addition, the Bangestan Group demonstrates the uplifting of the Burgan-Azadegan high during the deposition of the Bangestan Group by thinning along the crest [46].

The activity of the Burgan-Azadegan high is deducted from a structural cross-section, which it orthogonally crosses the Azadegan Anticline. This cross-section is horizontally flattened at the top Bangestan Group level from Ilam to Kazhdumi Formations. Other horizons are correspondingly shifted. The flattened cross-section shows that the uplifting of the Burgan-Azadegan high continued in the Late Cretaceous and Tertiary [43-44].

The Azadegan dome is a complex horst. Seismic data of the Azadegan structure shows steep faulting in the core of the anticline. These faults die up in the upper Jurassic Gotnia Formation (Figure 2). Drill-hole and seismic data from the Azadegan anticline demonstrate unconformities and erosional surfaces due to the uplifting of basement-cored horsts. For example, incised channels in the top Cenomanian-Turonian Sarvak Formation indicate erosion of the anticline crest in the Upper Cretaceous [43,47]. The thinning of the Mid-Cretaceous Bangestan Group and the Late Cretaceous Gurpi Formation in the crest reflects the Azadegan Anticline's activity of the Azadegan Anticline during the Mid. and Late Cretaceous [43-45]. The onlapping reflectors, especially on the western flank, and thinning of the layers above the crest indicate the uplift of the Azadegan high during the upper Cretaceous. The geological interpretation of the Azadegan high notes is that the steep faults die up into the upsection [43].

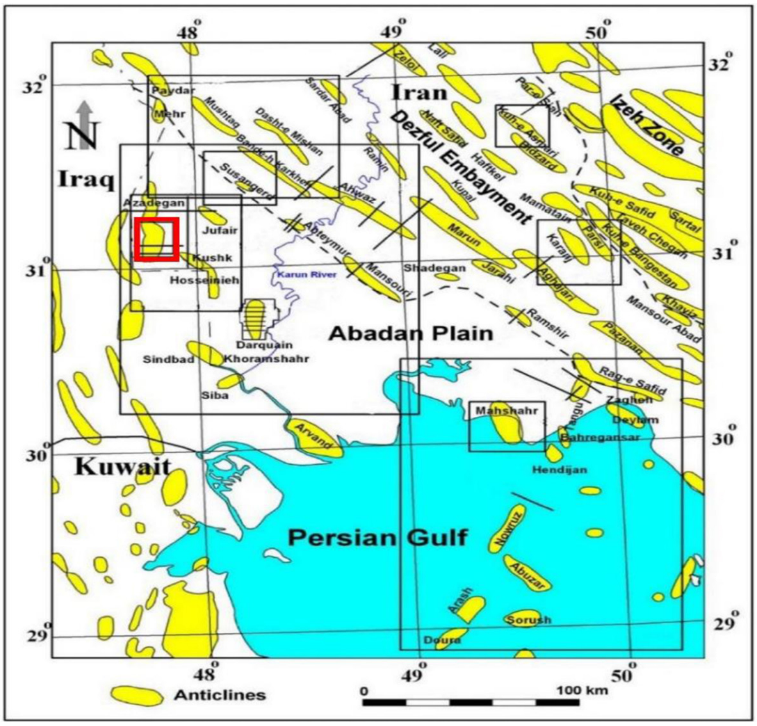

Fig. 1 Structural map of the Abadan Plain. Major anticlines appear as elongated domes. The location of maps and seismic profiles discussed are outlined [43].

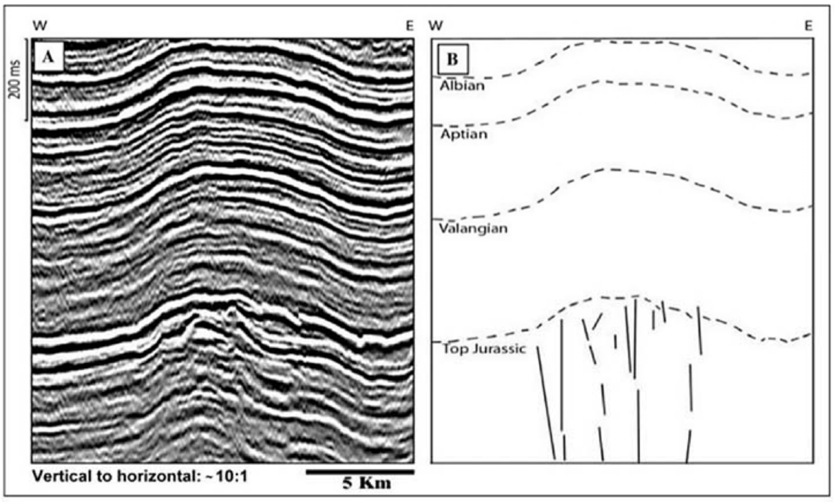

Fig. 2 Seismic profile across the Azadegan High shows a steep fault system in the Jurassic and underlying sedimentary rocks [43].

The seismic profile through the Azadegan high shows the channel-type reflector pattern above the Turonian strata. The incised channels show that the main activity of the Azadegan high led to the post-Turonian sea-level low stand [43-44].

Characteristics of reservoir formations in the South Azadegan Field

The reservoir formations of the south Azadegan Field include seven Formations, Pabdeh, Gurpi, Ilam, Sarvak, Kazhdumi, Gadvan, and Fahliyan, which will be briefly mentioned below:

Pabdeh Formation

Based on the correlation of seismic interpretation and drilling data, the Pabdeh Formation has a thickness of 272 meters in the A-001 well. It is composed of limestone with low permeability, but it could be a reservoir formation in three areas where permeability was increased. However, the entire Pabdeh Formation was considered a unit for volumetric calculations. Due to the similarity of the seismic horizon of the above formation with the Asmari horizon, during the construction of geological layers in the Petrel software, it is jointly considered with the Asmari Formation as the single layer of Asmari-Pabdeh. In the structural geological model, the average thickness of the Asmari and Pabdeh Formations is 727.8 meters [45].

Gurpi Formation

The Gurpi Formation is 255.4 m thick limestone in the A-001 well. Oil is present throughout but only in a few discrete intervals. There is a good reservoir. For volume calculations, the Gurpi Formation, with an average thickness of 368.4 meters, and the Tarbur member at its end, with an average thickness of 223.8 meters, were considered.

Ilam Formation

Ilam is composed of limestone; according to seismic interpretation, its thickness is 83.5 meters in the A-001 well, and the average thickness is 122.5 meters in the structural model. Due to the similarity of the seismic horizons of the Laffan and Sarvak Formations, this formation becomes thicker in the south, which makes it difficult to interpret and find the top of the Sarvak Formation.

Sarvak Formation

Sarvak's calcareous Formation is the main reservoir of Azadegan. Its thickness is 605 meters in A-001 well with a hydrocarbon column of 200 meters. The water-oil contact surface is observed at a depth of 2874 meters. The average thickness of the structural model is 656.4 meters.

Kazhdumi Formation

The Kazhdumi Formation is mainly composed of shale and marl, but it has an 18.5 m thick sandstone reservoir towards the base of the formation. This sandstone unit may thicken towards the south of the field. The contact surface of water and oil has been observed at 3502.5 meters for the Kazhdumi sandstone reservoir. The geological model's average thickness of the above formation is 225.8 meters.

Gadvan Formation

The Gadvan Formation consists mainly of shale and limestone but contains a 48.5 m high sandstone, which, like the Kazhdumi Sandstone, may thicken to the south of this field. The average thickness of the Gadvan formation is 186 meters, and 123.5 meters in the lower part of the Khalij member.

Fahliyan Formation

The Fahliyan Formation consists of thick clayey limestones with poor reservoir quality containing heavy oil. In the south of the Darquain field, the Fahliyan Formation has good reservoir conditions, and reservoir quality may improve in Azadegan to the south [45-46]. The average thickness of the Fahliyan Formation in the upper part is 151.7 meters, and in the lower part up to the beginning of the Gotnia Formation, it is 850.4 meters thick on average [47-48]. The general geological column of the Azadegan Field is shown in Figure 3.

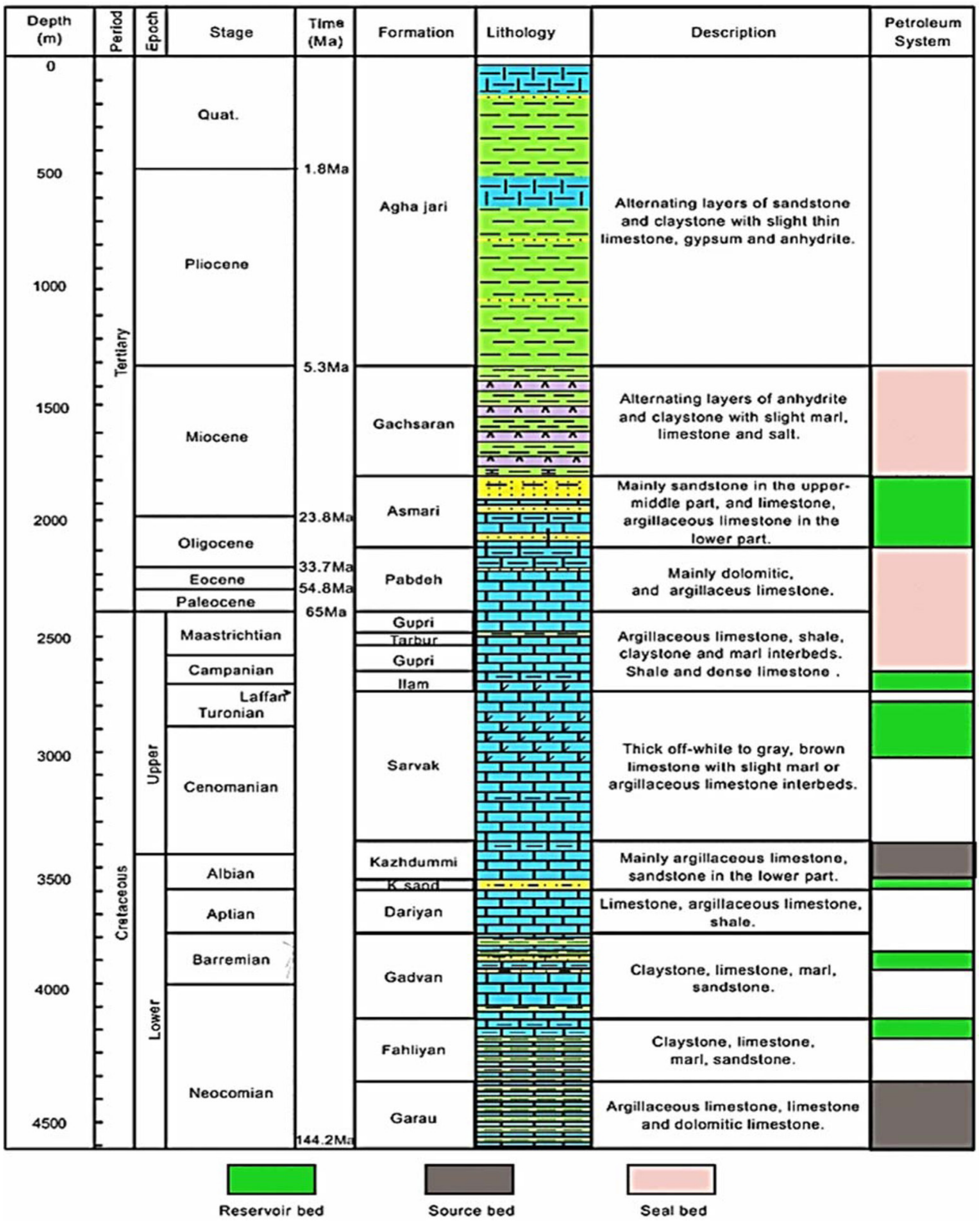

Fig. 3 General Geological Column of Azadegan Field [42].

Material and Methods

Overburden Pressure Cube

Calculating the overburden and effective pressure is necessary for calculating the pore pressure. First, the overburden pressure cube is calculated by integrating the average density value (from the surface to the desired depth). One of the most famous relationships used in seismography to make the relationship between velocity and density is the Gardner relationship and the Amoco experimental relationship. In Gardner's method, first, the logarithmic diagram of the completed cubes of the density logs is plotted relative to the compression velocity logs (Figure 4), and the logarithmic relation obtained becomes the exponential Relation 2.

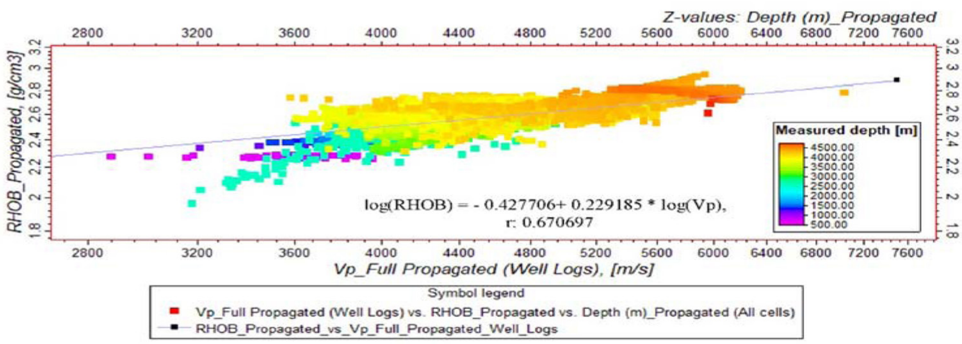

Fig. 4 Logarithmic relation of density cube graphs to compression velocity of South Azadegan basin.

$$\rho = aV_p^{\,b} \tag{2}$$

In another method, the mean density is obtained through the Amoco experimental relation based on depth in meters.

$$\rho_{avg} = \frac{\left(16.3 + \frac{3.281*Depth}{3125}\right)^{0.6}}{8.354} \tag{3}$$

Due to the high correlation coefficient between the Gardner relation and the Amoco relation of 92.4%, the use of the density cube obtained from the Gardner relation coefficients is approved due to its higher accuracy. The relationships used to construct each of the cubes are provided in the Petrol 2016 conditional programming language; Final Overburden pressure cube (in psi) based on average density and depth is shown in Figure 5.

To calculate the overburden pressure, given that the product of density (grams per cubic centimeter) in gravity acceleration (9.81 meter per second squared) at depth (meters) is obtained in kilopascals, to calculate the pressure in pounds per square inch (psi) requires a conversion factor of 145.038/1000, so the relationship is as follows:

$$P_{0.B} = \frac{9.81*\rho_{vag}*Depth*145.038}{1000} \tag{4}$$

Effective Pressure Cube

MDT and DST pressure test data of the studied field generally start from Sarvak Formation and continue to Gotnia Formation, but pressure data in the upper formations are minimal (Figure 6). Therefore, considering obtained data from these 23 wells, using the proposed methods such as sequential Gaussian simulation (SGS) and inverse distance weighted (IDW) was possible.

Therefore, the initial modeling of the effective pressure was done using three methods of Bowers: velocity cube (co-kriged with acoustic impedance), SGS (co-kriging with velocity cube), and IDW method. In the next step, the results of the primary pressure cubes using a neural network are fully propagated by the feed forward-back propagation (FFBP-NN) method, and cube determination of accepted data by the principal component analysis (PCA) method was done. Therefore, the best method with the highest correlation coefficient with initial MDT data as the basic method for the final calculation of formation pressures has been chosen (Table 1). To modify the model, five information layers, including formation gamma, compressional velocity, seismic acoustic impedance inversion (AI), density, and overburden pressure, had the highest linear convergence with the initial effective pressure models were used.

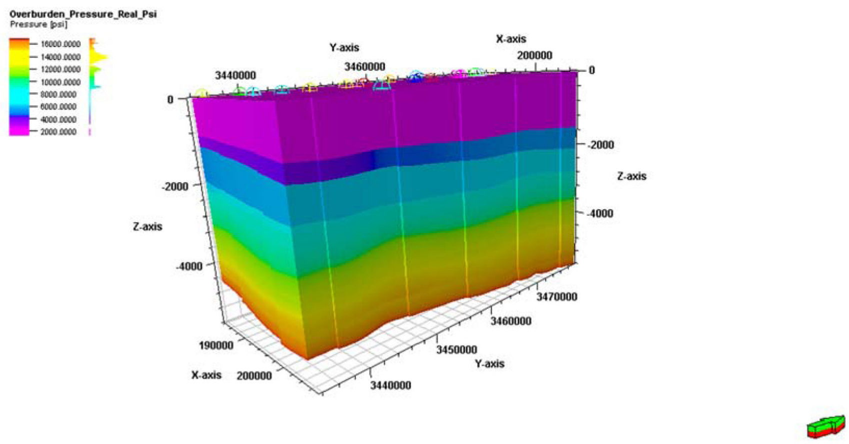

Fig. 5 Final Overburden pressure cube (in psi) based on average density and depth.

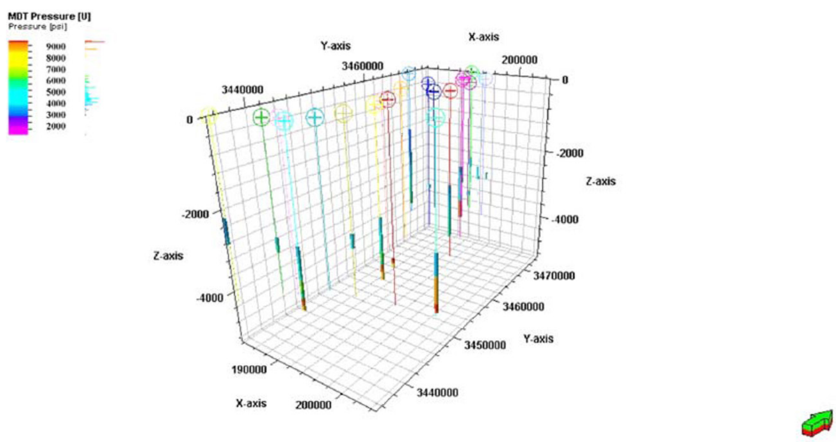

Fig. 6 Initial scale-up model resulting from MDT well logging data and DST pressure tests.

Table 1 Correlation coefficients (r) of the main components analysis (PCA) of the final neural network model of effective pressure obtained from the initial models by Bowers, SGS, and IDW methods.

Correlation Coefficients of Bowers, SGS and IDW Method	PC0	PC1	PC2	PC3	PC4
GR Cube	0.0677	0.9523	0.2282	0.1475	0.1214
Seismic acoustic impedance Inversion (AI) cube	-0.8173	-0.2393	0.5137	-0.0411	-0.0955
Vp (Well Logs) cube	-0.8681	-0.3534	-0.0891	0.2105	0.2630
RHOB Density Cube	-0.8660	0.3069	-0.2376	0.2135	-0.2320
Overburden Pressure cube	-0.8307	0.3625	-0.1460	-0.3901	0.0709
Eigenvalue	2.8662	1.3146	0.4017	0.2656	0.1519
Contribution (%)	57.32	26.29	8.03	5.31	3.04
Cumulative Contribution (%)	57.32	83.62	91.65	96.96	100.00

Based on the comparison of the three methods, in the effective pressure cube made with the neural network based on the initial SGS model with 30 iterations, the training error values of 1083.53, test error of 1083.64, and relative error of 0.536 have been calculated. It has the lowest error values compared to the other two methods.

Pore Pressure Cube

Based on the Terzaghi relationship (Equation 5), each of the completed effective pressure cubes (P_{eff}) is deducted from the overburden pressure cube ($P_{O.B}$). Furthermore, correlating the pore pressure cubes (Ppore) made with the initial effective pressure data for different formations in all three methods has been examined for different formations. In the Bowers method, the correlation coefficients in the Tarbur member of Gurpi Formations with 0.93, Gadvan with 0.36, and Khalij member with 0.27 show higher values. However, applying the SGS method, the coefficients correlation overall stand in higher values, as in Tarbur member of Gurpi Formation with 0.73, Ilam with 0.47, Sarvak with 0.48, Kazhdumi with 0.14, Dariyan with 0.27, Gadvan with 0.14, Khalij member of Gadvan Formation with 0.19, Upper Fahliyan with 0.22, and lower Fahliyan to Gotnia is -0.57 (due to the reduction pressure trend in the lower Fahliyan Formation). Also, in the IDW method, the correlation coefficients are lower than SGS and Bowers methods, and in some cases, they are negative. Thus the SGS model (co-kriged with VP and AI cubes), which has the highest correlation coefficient, is confirmed to calculate the final pore pressure gradient (Figure 7 and Table 2).

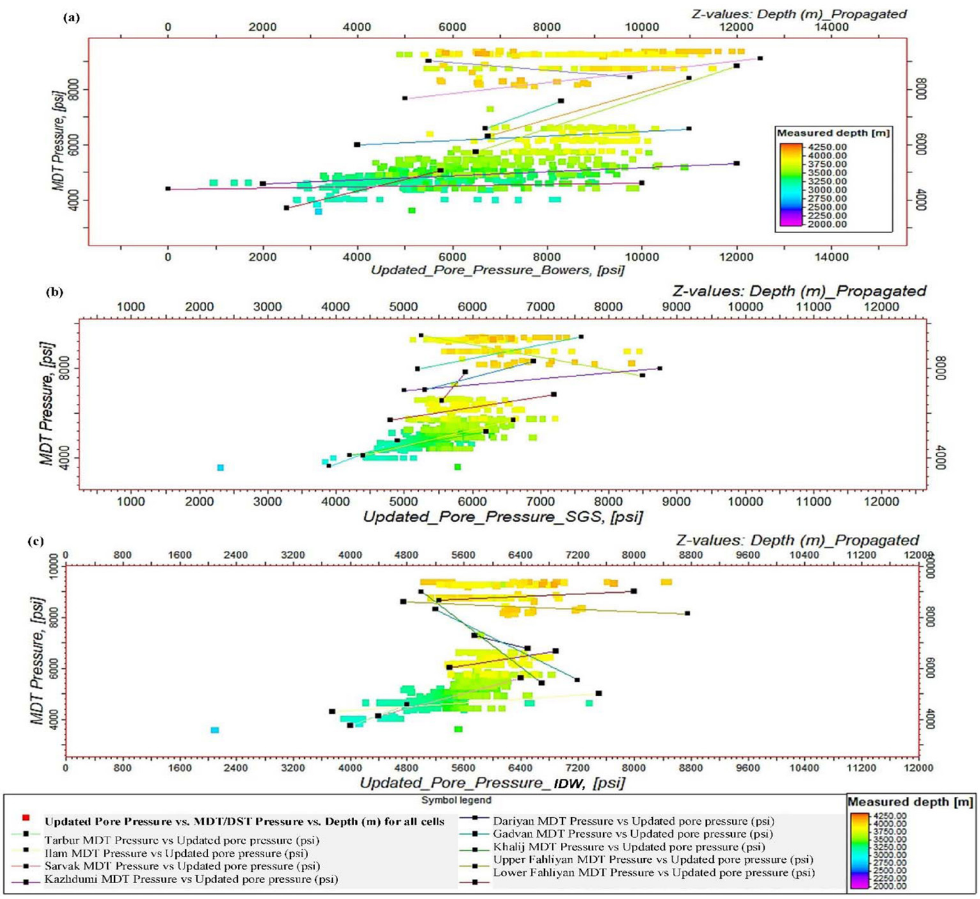

Fig. 7 Correlation coefficients of initial data of MDT/DST effective pressure and pore pressure models obtained from a) Bowers, b) SGS and co-kriging with acoustic impedance obtained from seismic inversion, and c) IDW methods.

Table 2 Correlation coefficients of formation pore pressure cubes of studied field using neural network based on Bowers, SGS, and IDW models with primary MDT data.

Formation	Correlation coefficient of Pore pressure and Primary MDT data		
	Bowers method	SGS method	IDW method
Tarbur (member of Gurpi)	0.93	0.73	0.57
Ilam	0.12	0.47	0.34
Sarvak	0.24	0.48	0.48
Kazhdumi	0.07	0.14	0.09
Dariyan	0.19	0.27	-0.1
Gadvan	0.36	0.14	-0.4
Khalij (member of Gadvan)	0.27	0.19	-0.49
Upper Fahliyan	0.21	0.22	-0.06
Lower Fahliyan	-0.25	-0.57	0.1
Total MDT Data	0.58	0.57	0.44

$$P_{pore} = P_{0.B} - P_{eff} \quad (5)$$

Data Validation of Final Pore Pressure Model Using Updated Bowers Coefficients

For data validation of final pore pressure, the effective pressure data in each formation of the final cube are compared with the compressional velocity cube data for the same formations. Finally, the Bowers relation coefficients are recalculated (Figure 8 and Table 3).

Fracture Pressure Cube

For determining the formation fracture pressure, Poisson's ratio (υ) has been calculated by having the data of the final shear velocity as well as the completed compressional velocity. Afterward, it has modeled based on the ratio of compressional to shear velocity by Relation 6 in the form of a log and, finally, as a cube. Poisson's ratio values are generally between 0.2 and 0.1, which is acceptable. Finally, by overburden pressure, pore pressure, and Poisson's ratio and using Eaton's equation, the formation fracture pressure is calculated according to Equation 7:

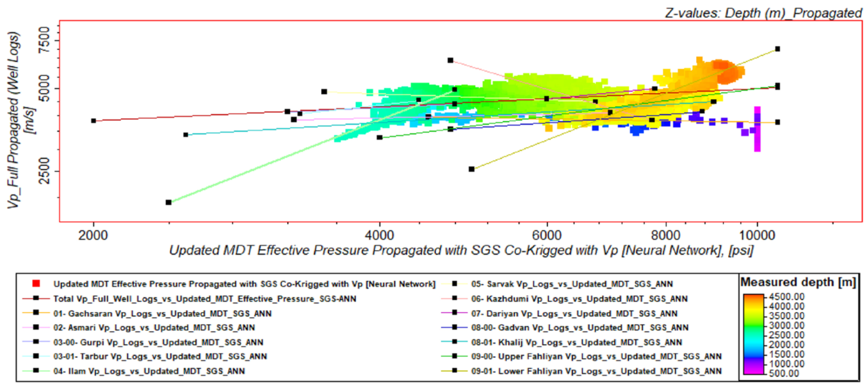

Fig. 8 Correlation coefficients of the final effective pressure model with the velocity cube model (update of the Bowers relation coefficients) in the whole field.

Table 3 Parameters and correlation coefficients (r) of final Effective Pressure and Compressional Velocity cubes for updated Bowers relations in different formations of the studied field.

Formation	$V=aP_{eff}^{b}$	r
Gachsaran	A=6112.23, B=-0.052	-0.17
Asmari	A=2006.3, B=0.077	0.32
Gurpi	A=1055.9, B=0.1682	0.45
Tarbur (Member)	A=151.68, B=0.405	0.26
Ilam	A=0.043, B=1.374	0.71
Sarvak	A=13720, B=-0.127	-0.27
Kazhdumi	A=33078.3, B= -1.025	-0.65
Dariyan	A=290.35, B=0.318	0.44
Gadvan	A=439.7, B=0.247	0.25
Khalij (member)	A=613.49, B=0.218	0.19
Upper Fahliyan	A=77.5, B=0.453	0.55
Lower Fahliyan	A=0.023, B=1.363	0.86
Total Field	A=1042.46, B=0.1705	0.38

$$\vartheta = \frac{(V_P^2 - 2V_S^2)}{2(V_P^2 - V_S^2)} \quad (6)$$

$$P_{Fraction} = (P_{Overburden} - P_{pore}) * (\frac{\vartheta}{1-\vartheta}) + P_{pore} \quad (7)$$

Results and Discussion

Results

Considering the methodology described in Materials and Methods, by converting Relation 2 to exponential, the equation becomes RHOB = 10 $^{(-0.427706)}$ VP $^{0.229185}$, so the Gardner relation coefficients are calculated as a = 0.38 and b = 0.23. Therefore, to calculate the average density using the average velocity cube, the check shot data and vertical seismic profiling (VSP) have been used to produce average velocity cube. Accordingly, the highest correlation coefficient between the final effective pressure cube, and the velocity cube is related to the lower Fahliyan Formation with 0.86 and Ilam with 0.71, which it indicates the high accuracy of the modeled data with the original data.

The maximum fluctuations of shear velocity are in the range of 2200 to 3000 meters per second (m/s), and the maximum is more than 3000 m/s at depths of more than 4200 meters (Figure 9).

Constructing of the Structural Geological Model Based on Seismic and Geological Data

As the range of the geological model network has been defined, the horizontal (I) and vertical (J) axes, and the number of network nodes, were added. Then, the three-dimensional structure of the field, along with the beginning, middle, and end levels of the network, was modeled by Petrel 2016 software. Finally, the layout of the wells was determined. In the next step, using the geometrical modeling section and the arithmetic seismic resampling method of Petrel software and determining the In-line and X-line ranges of the amplitude values, a seismic data cube with post-stack data has been created (Figure 10).

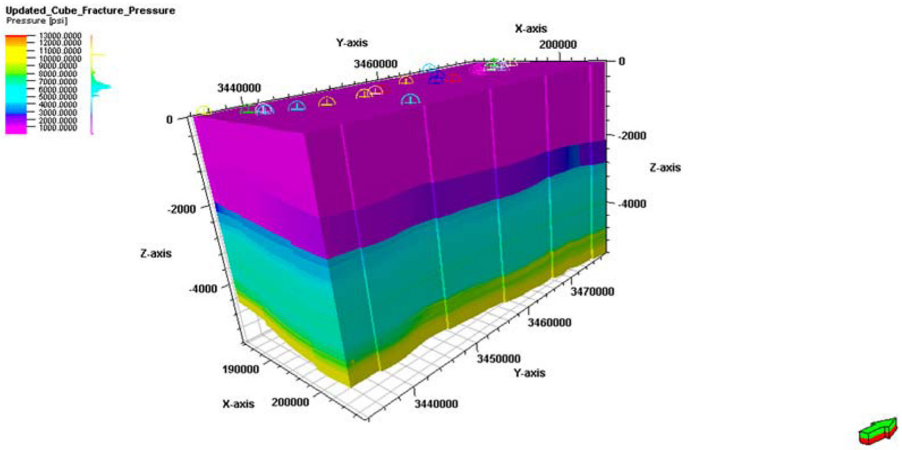

Fig. 9 Final formation fracture pressure cube based on final pore pressure cube, overburden pressure cube, and Poisson's ratio.

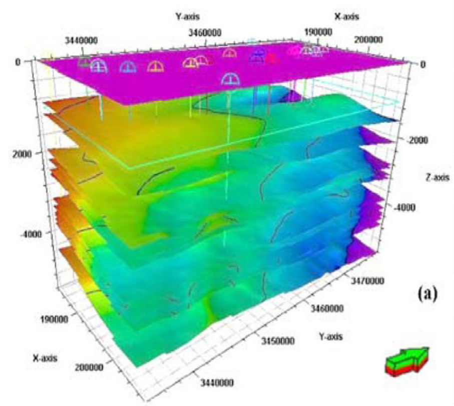

Geometry of Volume Base Model (VBM)			Inline	Crossline
Origin	183,540.30	3434410.05	2950	5012
I axis	205,731.90	3433719.97	2950	5900
J axis	184,938.96	3479388.03	4750	5012
Width (m)	22,202.32		J axis w h I axis Rotation	
Height (m)	44,999.72			
Rotation (degree)	-1.78			
Grid Increment				(b)
I Increment	150.02		Coarsening	1
J Increment	150		Nodes	149*302

Fig. 10 a) All depth-domain seismic horizons entered into the geological model of South Azadegan Field, b) Defining the geological network of the project along with I and J axes (field boundaries).

South Azadegan Field formations are modeled based on the interpretation of time-domain seismic horizons data and correlated with geological information obtained from exploratory drilling. Depth-domain seismic horizons have been constructed as separate surfaces from the surface Aghajari Formation to the Gotnia Formation. Due to the lack of complex fault systems in the area, the geological model has been built with a simple network of Petrel 2016 software (Figure 11).

Pore and Fracture Pressure Variations

Based on comparing histograms of pressure changes, due to the small changes between the minimum and maximum values of pore pressure and fracture pressure in Formations such as Kazhdumi and Gadvan at a rate of less than 200 psi, to design a drilling mud window, safe interval values to prevent well flow and formation loss of about 50 psi has been suggested. Based on the obtained results, the increase in pore and fracture pressures of the formation is quite noticeable with increasing depth, except for the lower Fahliyan Formation, in which, with an increasing depth, a decrease in pressure in this formation is seen. Based on the modeled pressure cubes, the maximum pore pressure of 10,000 psi in the Gadvan Formation to the upper Fahliyan Formation and the maximum fracture pressure of 13,000 psi in the Lower Fahliyan Formation to Gotnia have been obtained (Figures 12, 13 and Table 4).

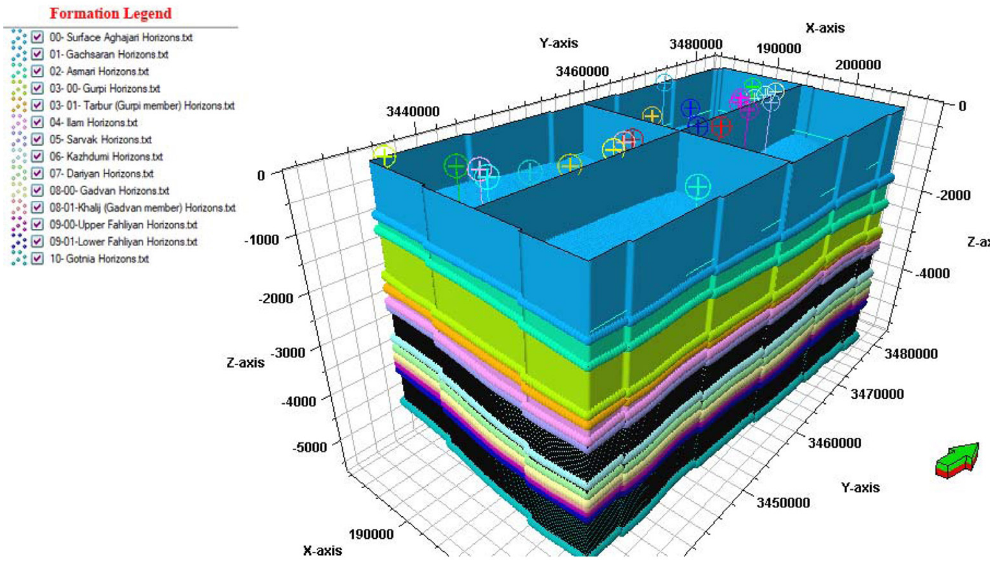

Fig. 11 Three-dimensional geological model of South Azadegan Field using seismic sections and drilling data along with the location of used wells.

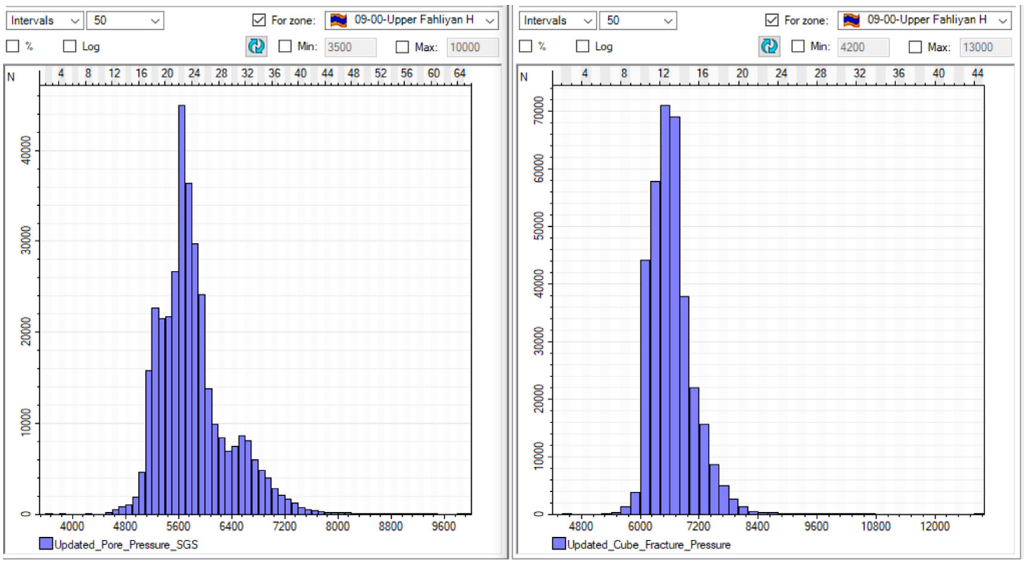

Fig. 12 Histogram of formation pressure changes a) pore and b) fracture in the upper Fahliyan Formation.

Table 4 Changes in pore and fracture pressures based on the modeling of formation pressures of South Azadegan Field.

Formation	Pore Pressure (psi)	Fracture Pressure (psi)
Aghajari	76.2-87.2	94-142
Gachsaran	10-440	80-640
Asmari and Pabdeh	100-3900	100-4900
Gurpi	2250-4700	2500-4900
Tarbur (Member)	3550-4900	3825-5125
Ilam and Laffan	4240-6160	4500-7550
Sarvak	4300-6550	4750-7550
Kazhdumi	4800-7100	5000-8200
Dariyan	5025-6425	5780-6680
Gadvan	4900-9900	5200-12600
Khalij (member)	4800-10000	5000-12600
Upper Fahliyan	3500-10000	4200-10000
Lower Fahliyan to Gotnia	5000-9700	5400-13000

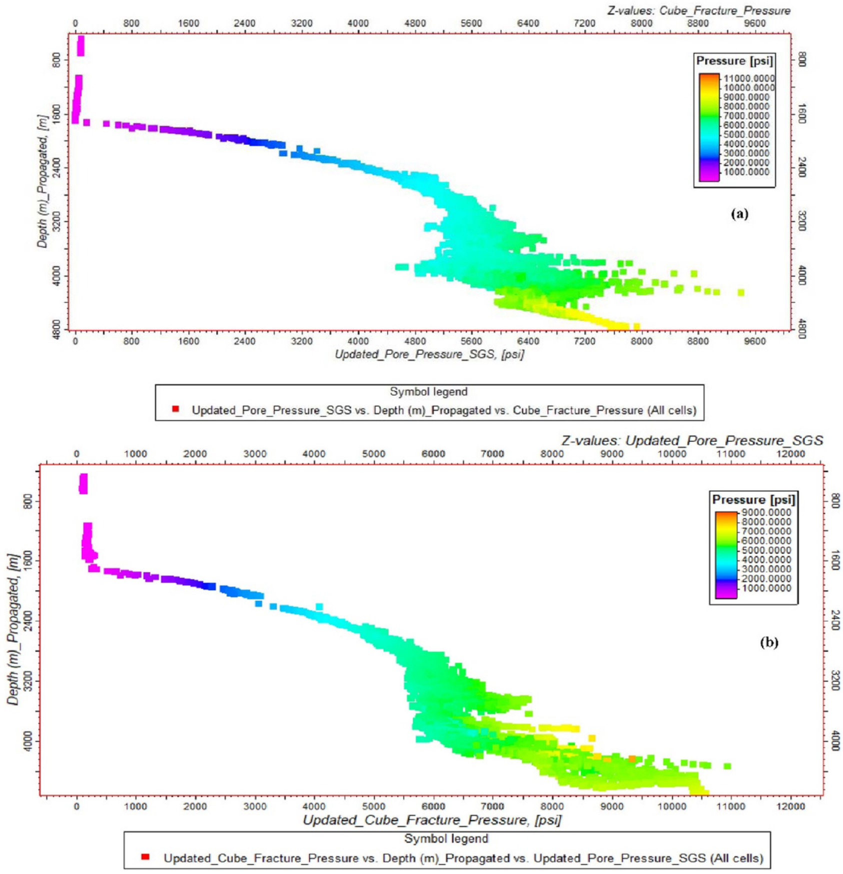

Fig. 13- a) model of pore pressure changes, b) fracture pressure of the formation to increase the depth in the south Azadegan Field.

Pore Pressure Gradient Model of Areas with Higher than Normal Pressure

According to the pore pressure gradient results in the final sequential Gaussian simulation (SGS) method, the studied field generally has a higher than normal pressure from the depth of 2000 meters down (except upper Fahliyan formation) in the range between 0.465 to 1 psi/ft. Areas with abnormal pressure are shown in Figure 14. Therefore, in the design stage of drilling mud windows, these areas have been considered to design the minimum mud weight.

Anisotropic Spatial Variation of Final Pore Pressure Cube

For evaluating anisotropy variations in the final pore pressure cube, experimental variograms with the Gaussian method were created in three directions: vertical, major horizontal azimuth of zero degrees, and minor azimuth of 270 degrees. In the vertical Variogram, the sill is 0.937, and in major and minor is 1. The anisotropy range based on Petrel 2016 software computations for vertical variogram range is 68 meters, and for major and minor directions is 11850 meters. Experimental calculations and anisotropy range are shown in Tables 5 and 6. Also, semi-variograms are shown in Figure 15.

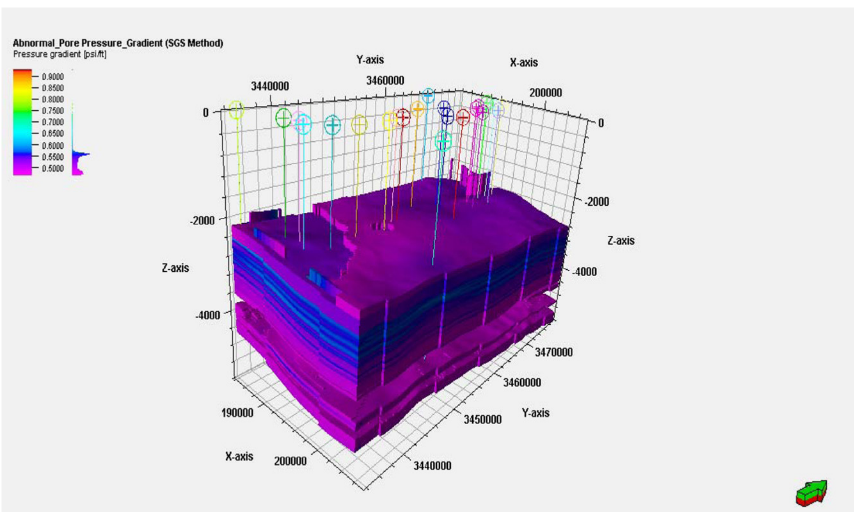

Fig. 14 Area with higher than normal pore pressure by SGS method in the studied field.

Table 5 Experimental variogram computation for final pore pressure cubes.

Direction	Azimuth	Dip	Number of lags	Lag distance	Search radius	Band width	Tolerance angle	Lag tolerance	Thickness
Vertical	NA	90	8	25	200	50	45	50	0.001
Major	0	0	8	250	2000	200	45	50	0.001
Minor	270	0	8	250	2000	200	45	50	0.001

Table 6 The results of Gaussian Variogram of the pore pressure cube obtained by combining SGS and co-kriging methods with acoustic impedance (AI), and FFBP-NN methods in the study field.

Direction	Nugget	Sill	Range	Number of Pairs	Anisotropy range (m)
Vertical	0.0633	0.937	937.56	13374251	Vertical: 68
Major azimuth 0	0	1	10000	11367363	Major direction:11850
Minor azimuth 270	0	1	10000	11058663	Minor direction:11850

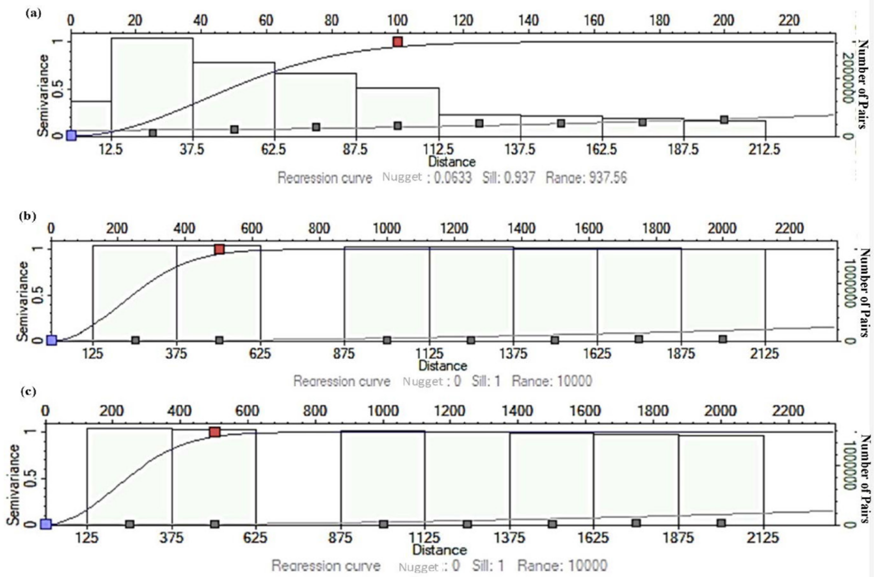

Fig. 15 Semi variogram of final Pore pressure Cube a) Vertical, b) horizontal major direction azimuth zero deg., c) minor direction azimuth 270 deg.

Discussion

The general formula of the Grade-volume fractal method is as follows (Equation 8):

$$V\left(\geq \rho\right) \propto \rho^{-D} \quad (8)$$

In this case, V is the volume that includes equal and more grades (ρ) in the studied deposit, and D is the fractal dimension. In this research, a new challenge has been done to study the effective, pore and fracture pressures by the fractal formation pressure-volume (P-V) method.

Value-number Fractal Model for the Effective Pressure of the Initial Data

Preliminary studies of the fractal model based on the available data include the presentation of the effective pressure-number (P-N) fractal model based on the change of Relation 9 as follows:

$$N\left(\geq P_{eff}\right) \propto P_{eff}^{\ -\beta} \quad (9)$$

In this relation, N contains the number of samples of effective pressures greater than and equal to P_{eff}, and β is the fractal dimension. Based on this, the average available MDT effective pressure log and DST pressure test data for Ilam to Fahliyan Formations are calculated. After sorting from large to small, the logarithm of effective pressure data and the number of data are calculated. Its diagram is presented in Figure 16 accordingly.

Based on the preliminary results, the effective pressure data has three breaking points at 4677, 4786, and 8511 psi, indicating four main pressure regimes or four formations with different pressures between Ilam and Fahliyan Formations. Next step was to complete the modeling of the final pressure cube data of the south Azadegan Field.

Value-volume Fractal Model for the Final Data Cube of the South Azadegan Field

Due to the high volume of about 1.5 million data rows (every 15 cm depth change, one data cube cell), the data at intervals of 1000 Meters have been analyzed. The results will be presented as pressure-volume (P-V) models based on Equation 10.

$$V\left(\geq P\right) \propto P^{-\beta} \quad (10)$$

V includes the sample volume of larger and equal formation pressures (P) in this relation, and β is the fractal dimension.

The division of South Azadegan Field based on the average cubic thickness of geological layers using Petrel 2016 software is shown in Table 7. Based on the average thickness divisions of the geological models, each of the Aghajari, Asmari, Pabdeh, Sarvak, Khalij member, and Sargelu Formations are located in the common parts of the two intervals of fractal models. Therefore, each model calculates the number of its data cells separately.

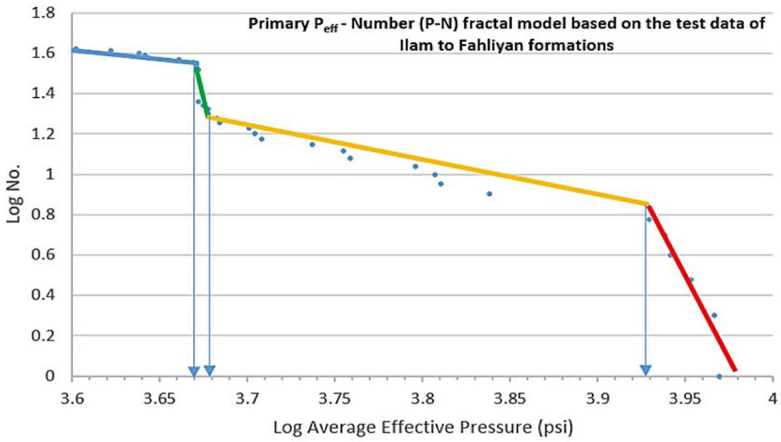

Fig. 16 Primary effective pressure- Number (P-N) fractal model based on the average MDT and DST data of Ilam to Fahliyan reservoir Formations.

Table 7 Division of South Azadegan Field based on the average cubic thickness of geological layers (using Petrel 2016 software).

Row	Formation	Formation Top (m)	Formation Base (m)	Average Thickness (m)	Dominant Lithology	Number of data cubes
1	Aghajari	0	1272.3	1272.3	Marl and sandstone	14,090
2	Gachsaran	1272.3	1630.65	358.35	Anhydrite and Claystone	7,571
3	Asmari and Pabdeh	1630.65	2368.25	737.6	Sandstone and Limestone	17,579
4	Gurpi	2368.25	2590.05	221.8	Limestone	26,650
5	Tarbur (Member)	2590.05	2757.85	167.8	Limestone and marl	93,179
6	Ilam and Laffan	2757.85	2866.05	108.2	Limestone and claystone	64,678
7	Sarvak	2866.05	3506.9	640.85	Limestone	382,420
8	Kazhdumi	3506.9	3733.95	227.05	Shale, Limestone and Sandstone	150,607
9	Dariyan	3733.95	3896	162.05	Limestone and marl	134,788
10	Gadvan	3896	3966.55	70.55	Marl, shale and limestone	85,320
11	Khalij (member)	3966.55	4071	104.45	Sandstone and Limestone	139,131
12	Upper Fahliyan	4071	4228.05	157.05	Limestone	190,818
13	Lower Fahliyan	4228.05	4589.1	361.05	Limestone	199,299
14	Garau	4589.1	4783	193.9	Limestone and claystone	75,612
15	Gotnia	4783	4931	148	Anhydrite and limestone	45,221
16	Najmeh	4931	4959	28	Anhydrite and limestone	6,678
17	Sargelu	4959	5068	109	Limestone and shale	17,858
18	Alan	5068	5107	39	Anhydrite and limestone	3,900
19	Muss	5107	5199	92	Limestone	7,089
20	Neyriz	5199	5590	391	Limestone and anhydrite	7,873

Because the effective pressures did not change significantly in the surface range up to 1000 m, its amount-volume (P-V) fractal model could not be prepared. Fractal diagrams of the amount-volume obtained from the effective pressure cube (E.P-V) for distances of 1000 meters are drawn in five separate diagrams, and the relevant interpretation is made. In general, the breaking points of the diagram show the formation change. For example, in Figure 17-a, the fractal diagram of effective pressure-volume (P-V) related to the depth of 2000 to 3000 meters in the south Azadegan Field has three breaking points. They are related to the changes in four effective pressure regimes of the Asmari-Pabdeh, Gurpi, Ilam-Laffan, and Sarvak Formations. Also, in Figure 17- b, related to the depth of 4000-5000 meters, three breaking points are related to the four effective pressure regimes of Khalij members of Gadvan, Fahliyan, Garau, and finally, Gotnia to Sargelu Formations.

Also, fractal diagrams of the amount-volume obtained from the Pore pressure cube (P.P-V) for distances of 1000 meters are drawn in 6 separate diagrams from surface to 5590, and the relevant interpretation is made (Figure 18).

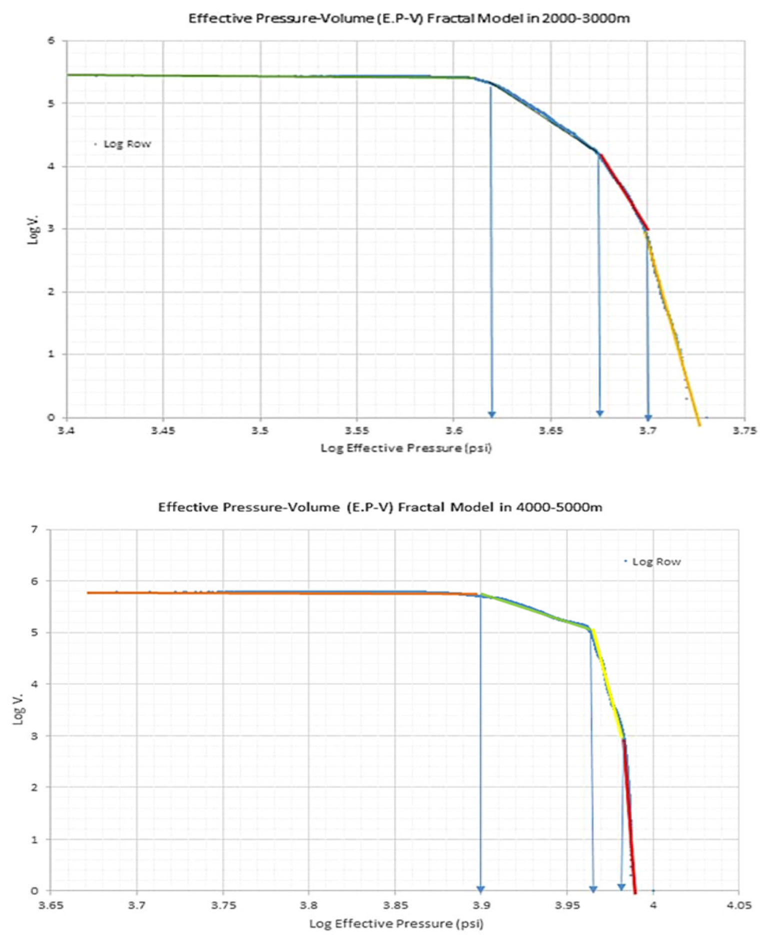

Fig. 17 Example of effective pressure fractal model a) depth 2000-3000 meters from South Azadegan Field (Asmari, Pabdeh, Gurpi, Ilam, and Sarvak Formations), b) 4000-5000 meters (Gadvan, Fahliyan, Garau, Gotnia, Najmeh, and Sargelu Formations).

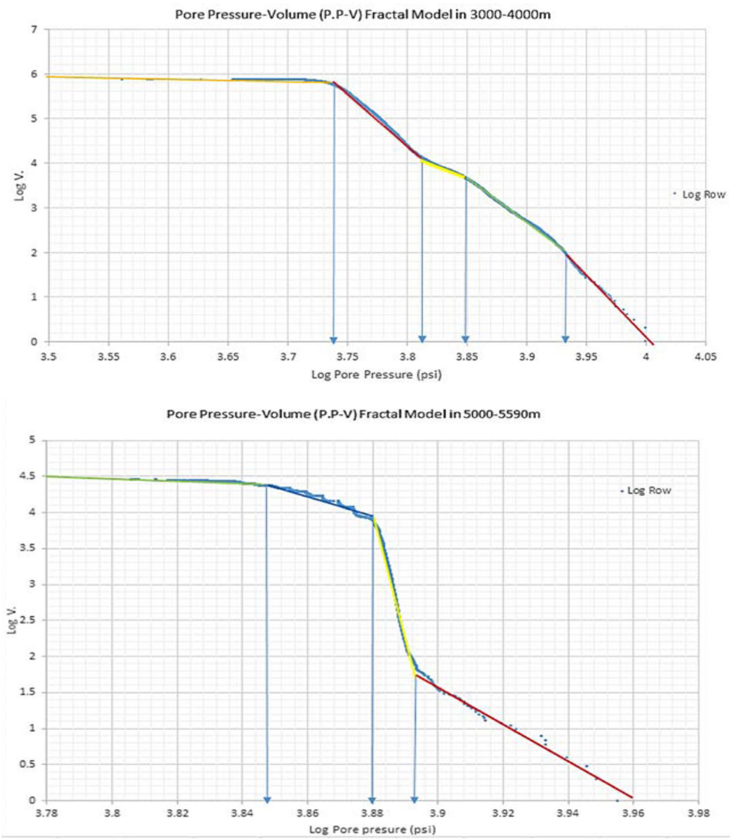

Fig. 18 Example of the fractal model of pore pressure-volume (P.P-V) a) depth 3000-4000 meters (Kazhdumi, Dariyan, and Gadvan Formations), b) depth 5000-5590 meters (Najmeh, Sargelu, Alan, Muss, and Neyriz Formations).

Finally, fractal diagrams of the amount-volume obtained from the Fracture pressure cube (F.P-V) for distances of 1000 meters, the same as effective and pore pressure diagrams, and the relevant interpretation is made (Figure 19).

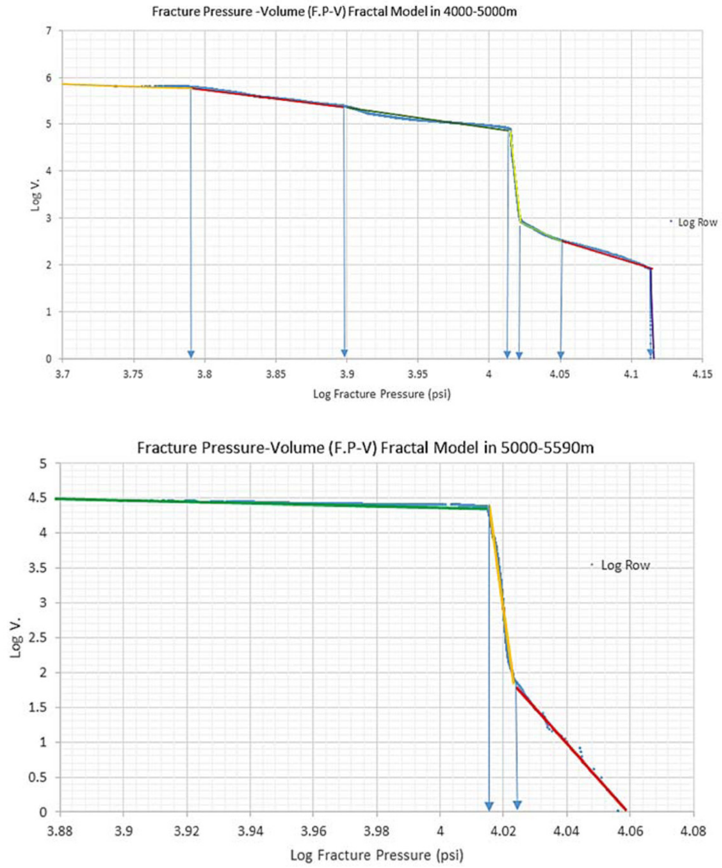

Fig. 19 An example of a fractal model of the amount-volume of fracture pressure (F.P-V) a) depth 4000-5000 meters (Gadvan, Fahliyan, Garau, Gotnia, Najmeh, and Sargelu Formations), b) depth 5000-5590 meters (Najmeh, Sargelu, Alan, Muss, and Neyriz Formations).

According to the comparison of breakpoints of pore pressure and formation fracture pressure regimes, from the surface up to 3000 m, the fracture pressure has one regime more than the pore pressure; at 4000-5000 m number of regimes is equal. At 3000-4000 m, the fracture pressure has two regimes less, and finally, at 5000-5590 m intervals, fracture pressure has one regime less than the pore pressure.

Matching the Pressure-volume Fractal Models and the Geological Model Using the Logratio Matrix

At this stage, the amount-volume fractal diagrams and determining the breakpoints and number of data of each interval as a mathematical model were completed. Afterward, based on the changes in the formation and lithology of the above intervals (geological model), the Logratio matrix was calculated for each effective pressure model. They were used to determine the highest correlation with the lowest error.

Correlation of Effective Pressure Fractal Model and Geological Model Using the Logratio Matrix

Based on the division of effective pressure regimes at depths of 1000 to 5590 meters into 24 different pressure regimes and determining the dominant geological model of each regime (including 15 pure limestone intervals, two limestones and marl intervals, two sandstone and limestone intervals, and two marl and sandstone intervals), Logratio matrices are calculated separately. Also, the lithology of surfaces up to 1000 m has small changes in marl and sandstone. Therefore, the Logratio matrix calculation has been omitted.

Accordingly, in the dominant limestone ranges, the highest overall accuracy (OA) of 0.78 in the pressure range of less than 5495.4 psi at depths of 3000-4000 meters is related to the Kazhdumi to Khalij member of the Gadvan Formation. Furthermore, the lowest OA of 0.27 in the pressure range between 9225.7 to 9549.9 psi is related to the Khalij member to Sargelu Formations at depths of 4000-5000 meters. Also, the highest overall accuracy of all geological ranges related to marl and sandstone at depths of 1000-2000 meters is 0.94. The table of error values and the overall accuracy of effective pressure intervals, with an example of the relevant Logratio matrix, is presented below (Table 8).

Correlation of Pore Pressure Fractal Model and Geological Model Using the Logratio Matrix

Also, based on the division of pore pressure regimes in depths of 1000 to 5590 meters into 24 different interval regimes and determining the dominant geological model of each regime (including 17 intervals of pure limestone, two intervals of limestone and marl, and five intervals of sandstone and limestone), Logratio matrices are calculated separately.

Table 8 Logratio matrix of the mathematical model (effective pressure less than 5495 psi) and geological model (dominant limestone) of 3000-4000 m interval.

		Geological Model (Pure limestone)			
		Inside zone		Outside zone	
Mathematical Model (Effective pressure less than 5495.4 psi)	Inside zone	True Positive (A)	149173	False Positive (B)	1223
	Outside zone	False Negative (C)	159609	True Negative (D)	411342
		Type I Error: C/(A+C)	0.5169	Type II Error: B/(B+D)	0.0030
		Overall Accuracy: (A+D)/(A+B+C+D)			0.777

Correlation of Pore Pressure Fractal Model and Geological Model Using the Logratio Matrix

Also, based on the division of pore pressure regimes in depths of 1000 to 5590 meters into 24 different interval regimes and determining the dominant geological model of each regime (including 17 intervals of pure limestone, two intervals of limestone and marl, and five intervals of sandstone and limestone), Logratio matrices are calculated separately.

Accordingly, in the dominant limestone intervals, the highest overall accuracy (OA) of 0.74 in the pore pressure range of less than 5248.1 psi at depths of 2000-3000 meters related to the Asmari to Sarvak Formations and the lowest to the extent of 0.31 in the pore pressure range between 6918.3 to 7498.8 psi is related to Khalij member of Gadvan to Sargelu Formations at depths of 4000-5000 meters.

In the dominant limestone and marl intervals, the highest OA of 0.57 in the pore pressure range of 7079.5 to more than 8511.4 psi is related to the Kazhdumi to Khalij member Formations at depths of 3000-4000 meters.

Finally, in the sandstone and limestone intervals, the highest OA of 0.79 in the pore pressure range of 1122 to 2290.9 psi at depths of 1000-2000 meters is related to Aghajari to Pabdeh Formations. Therefore, the highest overall accuracy (OA) of all geological intervals is related to sandstone and limestone at depths of 2000-3000 meters by 0.79. The table of error values and the overall accuracy (OA) of the pore pressure intervals obtained from the respective Logratio matrices is presented below (Tables 9 and 10).

Table 9 Logratio matrix of Mathematical model of pore pressure greater than 7834 psi and the dominant geological model of limestone depth 5000-5590 meters.

		Geological Model (Pure limestone)			
		Inside zone		Outside zone	
Mathematical Model (Pore pressure more than 7834.4 psi)	Inside zone	True Positive (A)	6	False Positive (B)	56
	Outside zone	False Negative (C)	7083	True Negative (D)	21187
		Type I Error: C/(A+C)	0.9992	Type II Error: B/(B+D)	0.0026
		Overall Accuracy: (A+D)/(A+B+C+D)			0.7480

Table 10 Total error values and overall accuracy (OA) of the Logratio matrices of the pore pressure mathematical models and the dominant geological models in the south Azadegan Field.

Interval (m) and formation	Pore Pressure regimes	Mathematical Model (Pore Pressure-psi)	Geological Model (dominant Lithology)	Mathematical Analysis (Type I Error)	Geological Sampling (Type II Error)	Overall accuracy (OA)
1000-2000 Aghajari, Gachsaran, Asmari and Pabdeh	5	< 16.6	sandstone and Limestone	0.87	0.09	0.58
		16.6-63.1	sandstone and Limestone	0.92	0.89	0.10
		63.1-1122	sandstone and Limestone	0.72	0.02	0.69
		1122-2290.9	sandstone and Limestone	0.49	0.00	0.79
		> 2290.9	sandstone and Limestone	0.997	0.00	0.58
2000-3000 Asmari, Pabdeh, Gurpi, Ilam and Sarvak	3	< 4677.3	Limestone	0.84	0.09	0.63
		4677.3-5248.1	Limestone	0.10	0.87	0.32
		> 5248.1	Limestone	0.65	0.03	0.74
3000-4000 Kazhdumi, Dariyan, Gadvan and Khalij member	5	< 5495.4	Limestone	0.65	0.20	0.61
		5495.4-6456.5	Limestone	0.35	0.77	0.41
		6456.5-7079.5	Limestone	0.997	0.02	0.56
		7079.5-8511.4	Limestone and marl	0.995	0.01	0.57
		> 8511.4	Limestone and marl	0.999	0.002	0.57
4000-5000 Khalij member of Gadvan, Fahliyan, Garau, Gotnia, Najmeh and Sargelu	7	< 5754.4	Limestone	0.80	0.17	0.44
		5754.4-6918.3	Limestone	0.28	0.47	0.65
		6918.3-7498.9	Limestone	0.93	0.28	0.31
		7498.9-7762.5	Limestone	0.99	0.08	0.35
		7762.5-8912.5	Limestone	0.992	0.002	0.38
		8912.5-9549.3	Limestone	0.9958	0.00008	0.37
		> 9549.3	Limestone	0.9999	0.00	0.37
5000-5590 Najmeh, Sargelu, Alan, Muss and Neyriz	4	< 7046.9	Limestone	0.89	0.20	0.63
		7046.9-7585.8	Limestone	0.30	0.49	0.56
		7585.8-7834.3	Limestone	0.81	0.31	0.57
		> 7834.3	Limestone	0.999	0.003	0.75

Advantages of the Models

The effective and pore pressure models with the predominant limestone formations in the south Azadegan Field match about 75%. Thus, the advantages of the above model include minimizing the time and cost of drilling in new wells by using drilling mud suitable for the formations so that the depth and pressure of the formation are determined with high accuracy. Also, risks such as loss of circulation and well flowing are avoided, and the use of drilling mud, cement materials and additions, and casing pipes determined for each phase of drilling will be optimized.

Wellbore Stability Suggestion

Since the drill cores data for geo-mechanical studies are not there in the South Azadegan Field, it is suggested to study wellbore stability using information obtained from new wells. Therefore, analyzing the wellbore stability of a vertical well through the reservoir layers of the oil-bearing formations should be investigated. The safe drilling-fluid density range for maintaining wellbore stability could be determined and simulated using FLAC3D software, and a finite volume model could be established with drilled strata geo-mechanical features. The initiation of plastic conditions could be used to determine the safe mud weight window (SMWW) in specific layers. The effects of rock strength parameters, major stresses around the wellbore, and pore pressure on the SMWW could be investigated for new wellbores.

Conclusions

1- The effective pressure cube made with a neural network based on the initial model of SGS has the lowest values of relative error compared to the two methods of Bowers and the IDW. Therefore, the accuracy of the pore pressure cube resulting from the SGS model (co-kriged with VP and AI cubes) and the data obtained from this method are considered for the final pore pressure gradient.

2- The highest correlation between the final effective pressure cube and the velocity cube is related to the lower Fahliyan Formation with 0.86 and Ilam with 0.71, which indicates the accuracy of the modeled data with the original data.

3- Based on the modeled formation pressure cubes, the most changes in overburden pressure are in the range of 10-16 thousand psi, maximum pore pressure of 10,000 psi in Gadvan formation to Upper Fahliyan and maximum fracture pressure of 13,000 psi in lower Fahliyan Formation to Gotnia has been achieved.

4- According to the final pressure models, the increase in pore pressures and fracture of the formation is quite noticeable with increasing depth, except for the lower Fahliyan Formation, which with increasing depth, a decrease in pressure is seen in this formation.

5- Due to the small changes between the pore pressure and fracture pressure in formations such as Kazhdumi and Gadvan at a rate of less than 200 psi, to design a drilling mud window, safe interval values of about 50 psi to prevent well flow and formation loss has been suggested.

6- In the Final Ppore cube's vertical Variogram, the sill is 0.937, and in major and minor is 1. The anisotropy range for the vertical variogram range is 96 meters, and for major and minor directions are the same as each other equal to 11850 meters.

7- Based on the preliminary results of the fractal Value-Number (V-N) model, the effective pressure data has three breaking points at 4677, 4786, and 8511 psi, indicating four main pressure regimes or four formations with different pressures between the Ilam to Fahliyan Formations.

8- After the modeling of formation pressure, velocity, and other final cube data of the south Azadegan Field, due to the high volume of data rows by about 1.5 million (every 15 cm change in-depth, one cube cell data), has been completed, the data are arranged based on depth and analyzed for every 1000 meters in different formations.

9- Based on the Logratio matrix in the mathematical model of effective pressure and the geological model in the dominant limestone ranges, the maximum overall accuracy (OA) of 0.78 in the pressure range of less than 544.4 psi at depths of 3000-4000 meters is related to the Kazhdumi Formation up to the Khalij Member. Also, the highest value of OA of all geological ranges related to marl and sandstone at depths of 2000-1000 meters is 0.94.

10- Based on the Logratio matrix in the pore pressure cube of the mathematical model and the geological model in the dominant limestone ranges, the maximum overall accuracy (OA) of 0.74 in the pressure range of less than 5248.1 psi at depths of 2000-3000 meters is related to Asmari to Sarvak Formations. Also, the highest OA of all geological ranges related to sandstone and limestone at depths of 3000-2000 meters is 0.79.

Acknowledgment

The present study is from a PhD dissertation on Mining Engineering - Mineral Exploration from Islamic Azad University, South Tehran Branch, hosted by the Research Institute of Petroleum Industry (RIPI). The authors consider it necessary to express their sincere gratitude to the esteemed experts of the RIPI and Exploration Directorates of the National Iranian Oil Company (NIOC). They helped us to carry out and improve the quality of this research.

Conflicts of Interest

The authors declare that they have no known competing financial interests or personal relationships that could have appeared to influence the work reported in this paper.

Nomenclatures

AI: Acoustic impedance
DSI: Dipole sonic imager
DST: Drill stem test
MDT: Modular dynamic tester
FFBP-NN: Feed forward-back propagation neural network
IDW: Inverse distance weighted
OA: Overall accuracy
OB: Overburden pressure
PCA: Principal components analysis
r: Correlation coefficient
RFT: Repeat formation test
SGS: Sequential Gaussian simulation
VSP: Vertical seismic profiling
ZFTB: Zagros Fold-thrust belt structures
υ: Poisson's ratio

References

1. Maddahi A, Ghazi Nezhad S, Ismailpour S, Heydari M (2014) Feasibility study of exploiting four-dimensional seismic studies of Sarvak reservoir in Azadegan Field, Journal of Petroleum Research, 78: 117-126 (in Persian).
2. Adim A, Riahi M, Bagheri M (2018) Estimation of pore pressure by Eaton and Bowers methods using seismic and well survey data, Journal of Applied Geophysical Research, 4, 2: 267-275 (in Persian).
3. Poorsiami H (2013) Modeling the pore pressure of a hydrocarbon reservoir in southwestern Iran using well-logging data, Journal of Petroleum Research, 23, 74: 72-86 (in Persian).
4. Aghebati R (2008) Introduction of a field: Azadegan Field development plan, scientific Journal of Oil and Gas exploration and production, November, 51: 6-8 (in Persian).
5. Jindal N, Kumar Biswal A, Hemant Singh K (2016) Time-Depth Modeling in High Pore-Pressure Environment, Offshore East Coast of India, AAPG 2016 Annual Convention and Exhibition, Calgary, Alberta, Canada, June 19-22.
6. Haris A, Sitorus R J, Riyanto A (2017) Pore pressure prediction using probabilistic neural network: case study of South Sumatra Basin, Southeast Asian Conference on Geophysics, IOP Conf. Series: Earth and Environmental Science 126324 (526071879) 0012021.
7. Radwan A E (2021) Modeling pore pressure and fracture pressure using integrated well logging, drilling based interpretations and reservoir data in the giant El Morgan oil field, Gulf of Suez, Egypt, Journal of African Earth Sciences, 178, 104165, ISSN 1464-343X.
8. Radwan A E, Abudeif A M, Attia M M, Elkhawaga M A, Abdelghany W K, Kasem A A (2020) Geopressure evaluation using integrated basin modelling, well-logging and reservoir data analysis in the northern part of the Badri oil field, Gulf of Suez, Egypt, Journal of African Earth Sciences, 162, 103743, ISSN 1464-343X.
9. Radwan A E, Abudeif A M, Attia M M, Mohammed M A (2019) Pore and fracture pressure modeling using direct and indirect methods in Badri Field, Gulf of Suez, Egypt, Journal of African Earth Sciences, 156: 133-143, ISSN 1464-343X.
10. Amirzadeh M, Kamali M R, Nabi Bidehandi M (2013) Investigation of reservoir characteristics by performing seismic data conversion and seismic markers in Sarvak Formation in one of the oil fields in southwestern Iran, Journal of Petroleum Research, 23, 75: 20-29 (in Persian).
11. Amiri Bakhtiar M S, Zargar Gh, Riahi M A, Ansari H R (2017) Seismic inversion by spectral simulation in one of the oil fields in southwestern Iran, the third oil exploration geophysics seminar, Exploration Directorate of the National Iranian Oil Company, 70-74 (in Persian).
12. Castagna J P, Batzle M L, Eastwood R L (1985) Relationships between compressional-wave and shear-wave velocities in clastic silicate rocks, GEOPHYSICS, 50, 4: 571-581.
13. Castagna J P, Batzle M, Kan L (1993) Rock Physics:The link between rock properties and AVO response, In: Offset-dependet reflectivity - Theory and practice of AVO analysis, Castagna, Investigations in Geophysics, 8: 135-171.
14. Fatahi H, Askari M, Majdi Far S (2016) Estimation of shear wave velocity in one of the hydrocarbon reservoirs of southwest Iran using different well logs and a new intelligent combined method Journal of Advanced Applied Geology, 22: 35-43 (in Persian).
15. Rajabi M, Hazbeh O, Davoodi S, Wood D A, Soltani Tehrani P, Ghorbani H, Mehrad M, Mohamadian N, Rukavishnikov V S, Radwan A E (2022) Predicting shear wave velocity from conventional well logs with deep and hybrid machine learning algorithms, Journal of Petroleum Exploration and Production Technology, published online 1-24.
16. Bowers G (1995) Pore pressure estimation from velocity data: accounting for overpressure mechanisms besides undercompaction, SPE Drilling and Completion, 10, 2: 89-95.
17. Bowers G L (2002) Detecting high overpressure, The Leading edge, 21, 2: 174-177.
18. Liu Y, Zhang X, Guo W, Kang L, Yu R, Sun Y (2022) An approach for predicting the effective stress field in low-permeability reservoirs based on reservoir-geomechanics coupling, Processes, 10, 633.
19. Yin H, Cui H, Gao J (2022) Research on pore pressure detection while drilling based on mechanical specific energy, 10, 1481.
20. Zhong L, Zhu T, Hao T, Zhang X, Xiaopeng Wang X, Zhang L (2020) Prediction method of formation pressure for the adjustment well in the reservoir with fault. Journal of Physics: Conference Series. International Conference on Physics, Mechanics and Mathematical Science,1707, 012012.
21. Zhang Z, Sun B, Wang Z, Pan S, Lou W, Dalin S (2022) Formation Pressure Inversion Method Based on Multisource Information, SPE Journal, 27: 1287-1303.
22. Abdelaal A, Elkatatny S, Abdulraheem A (2022) Real-time prediction of formation pressure gradient while drilling Scientific reports, 12: 11318.
23. Darvishpour A, Cheraghi Seifabad M, Wood D A, Ghorbani H (2019) Wellbore stability analysis to determine the safe mud weight window for sandstone layers, Petroleum Exploration and Development, 46, 5: 1031-1038.
24. Lantuejoul Ch (2002) Geostatistical simulation models and algorithms, Springer-VerlagBerlin Heidelberg GmbH, ISBN, 978-3-662-04808-5, 256.
25. Kelkar M, Perez G (2002) Applied geostatistics for reservoir characterization, Society of Petroleum Engineers, ISBN, 978-1-55563-095-9, 264.
26. Bohling G (2007) introduction to geostatistics, Hydro-geophysics: Theory, Methods, and Modeling, Boise State University, Boise, Idaho, 1: 26.
27. Armstrong M, Galli A, Beucher H, LeLoc'h G, Renard D, Eschard R, Doligez B, Geffroy F (2011) Pluri-gaussian simulations in geosciences, Springer-Verlag Berlin Heidelberg GmbH, ISBN, 978-3-662-12718-6, 149.
28. Karami O, Fallah A, Shataei S, Latifi H (2018)

Assessment of geostatistical and interpolation methods for mapping forest dieback intensity in Zagros forests, Caspian Journal of Environmental Sciences, 16, 1: 71-84.
29. Mandelbrot B B (1985) Self-affine fractals and fractal dimension, Physica scripta, 32, 4: 257.
30. Hassanpour S, Afzal P (2013) Application of concentration–number (C–N) multifractal modeling for geochemical anomaly separation in Haftcheshmeh porphyry system, NW Iran, Arab Journal Geoscience, 6: 957–970.
31. Afzal P, Fadakar Alghalandis Y, Khakzad A, Moarefvand P, Rashidnejad Omran N (2011) Delineation of mineralization zones in porphyry Cu deposits by fractal concentration–volume modeling, Journal of Geochemical Exploration 108: 220-232.
32. Soltani F, Afzal P, Asghari O (2014) Delineation of alteration zones based on Sequential Gaussian Simulation and concentration–volume fractal modeling in the hypogene zone of Sungun copper deposit, NW Iran. Journal of Geochemical Exploration, 140: 64-76.
33. Pourgholam M M, Afzal P, Adib A, Rahbar K, Gholinejad M (2022) Delineation of iron alteration zones using spectrum-area fractal model and TOPSIS decision-making method in tarom metallogenic zone, NW Iran, Journal of Mining and Environment (JME), 13, 2: 503-525.
34. Kianersi A, Adib A, Afzal P (2021) Detection of effective porosity and permeability zoning in an oil field using fractal modeling, International Journal of Mining and Geo-Engineering, 55, 1: 47-56.
35. Farhadi S, Afzal P, Boveiri Konari M, Daneshvar Saein L, Sadeghi B (2022) Combination of machine learning algorithms with concentration-area fractal method for soil geochemical anomaly detection in sediment-hosted irankuh pb-zn deposit, Central Iran, Minerals, 12, 6: 689.
36. Kianoush, P, Mohammadi G, Hosseini SAK, Keshavazr Faraj Khah N, Afzal P (2022) Compressional and Shear Interval Velocity Modeling to Determine Formation Pressures in an Oilfield of SW Iran. Journal of Mining and Environment, 13, 3: 851-873..
37. Daneshvar Saein L, Rasa I, Rashidnejad Omran N, Moarefvand P, Afzal P (2012) Application of concentration-volume fractal method in induced polarization and resistivity data interpretation for Cu-Mo porphyry deposits exploration, case study: Nowchun Cu-Mo deposit, SE Iran, Nonliner Processes in Geophysics, 19: 431–438.
38. Yasrebi A B, Hezarkhani A, Afzal P (2017) Application of present value-volume (PV-V) and NPV-cumulative total ore (NPV-CTO) fractal modelling for mining strategy selection, Resources Policy, 53, 384-393.
39. Mahdizadeh M, Afzal P, Eftekhari M, Ahangari K (2022) Geomechanical zonation using multivariate fractal modeling in Chadormalu iron mine, Central Iran. Bulletin of Engineering Geology and the Environment, 81, 1: 1-11.
40. Carranza E J M (2011) Analysis and mapping of geochemical anomalies using logratio-transformed stream sediment data with censored values, Journal Geochem Explor, 110, 2:167–185.
41. Radwan A E (2022) Chapter Two - Three-dimensional gas property geological modeling and simulation, In Sustainable Geoscience for Natural Gas Subsurface Systems, Gulf Professional Publishing, 29-49.
42. Du Y, Chen J, Cui Y, Xin J, Wang J, Zhen Li Y, Fu X (2016) Genetic mechanism and development of the unsteady Sarvak play of the Azadegan oil field, southwest of Iran, Petroleum Science, 13: 34–51.
43. Abdollahie Fard I (2006) Structural models for the South Khuzestan area based on reflection seismic data, Ph.D. Dissertation in Geology Tectonics, School of Earth Sciences, Shahid Beheshti University, Tehran, Iran.
44. Abdollahie Fard I (2019) Abadan plain exploration potential evaluation project, GR 2480, Pore Pressure Analysis, NIOC Exploration Directorate, Published report in Farsi, Tehran, Iran, 5: 10.
45. Morgan P (1999) Azadegan Field Geophysical Interpretation Part 1, ConocoPhillips UK LTD, August 1999, Technical Report in English.
46. Abdollahie Fard I, Hassanzadeh Azar J (2002) Application of true dip and thickness attributes in seismic interpretation, Institute of Geophysics, Tehran University, Journal of the Earth and Space Physics, 28: 17-23 (In Persian).
47. Mokhtari M, Zandifar H, Abdollahie Fard I (1999) Seismic interpretation of top Sarvak Formation in Azadegan-Nir Kabir Area (SW Iran), National Iranian Oil Company, Exploration Directorate, Published report in Farsi.
48. Mohammadi M, Farhani M (2011) Evaluation report of the Jurassic horizon of the well Azadegan-10, National Iranian Oil Company, Exploration Directorate, General Directorate of Petroleum Engineering, 71.